The Problem of Atomic Hydrogen

T. M. Donahue

Paper presented at the Symposium on Aeronomy,

Cambridge, Mass.

August, 1965

to be published in the

Annales de Géophysique

Department of Physics

University of Pittsburgh

Pittsburgh, Pennsylvania

The Problem of Atomic Hydrogen

T. M. Donahue
Department of Physics
University of Pittsburgh
Pittsburgh, Pa.

ABSTRACT

14952

Observations of the Lyman α airglow from 1959 through 1965 indicate that there is a large diurnal variation of hydrogen in the earth's thermosphere and exosphere and that the abundance has changed markedly from solar maximum to solar minimum. The change is always toward more hydrogen with decreasing exospheric temperature as theory predicts. H_α measurements agree with this picture but H_α is an order of magnitude too bright. There is also an extra-terrestrial component in Lyman α. Recent calculations of the effect of lateral flow in the exosphere show that the vertical flux resulting will not wipe out the diurnal hydrogen bulge but will have a serious effect on the helium diurnal variation. Refinement of the escape problem calculations involving abandonment of a discontinuity at the base of the exosphere predict a factor of three reduction in escape rate and a larger solar cycle effect.

Author

I. INTRODUCTION

The distribution of hydrogen atoms in the earth's atmosphere has not yet been studied by means of mass spectrometric techniques. At present we are dependent for all of our information relating to its behavior on optical absorption and emission spectroscopy and on inferences drawn from the distribution of protons in the exosphere. This paper will review the status of the optical observations and discuss some recent theoretical advances toward an understanding of the processes which control the vertical distribution.

The optical observations fall into three classes: detection of the absorption profile produced in the broad Lyman α emission line of the sun by telluric hydrogen and measurement of the variation of the equivalent width of this absorption line as a function of the altitude of the detector; observation of the Lyman α radiation from the sun scattered resonantly by the earth's hydrogen; and observation of the Balmer α line resulting from absorption of solar Lyman β radiation by hydrogen and subsequent cascade radiation leading to Balmer α and Lyman α emission.

II. SOLAR INTENSITIES

In these measurements a knowledge of the effective intensity at the center of the solar lines is required if conclusions are to be drawn from the absolute intensity of the scattered radiation. In the absence of solar intensities that relate to the proper phase of the solar cycle it is necessary for interpretation of measurements to resort to data

pertaining to the variation in scattered intensity with altitude or with solar zenith angle. Thus far there have been only two measurements reported for the intensity at the center of the solar Lyman α line. Both were obtained by rocket borne spectrometers flown by the group working under Richard Tousey at NRL. One in July 1959[1] gave the central intensity as 4.7 ergs/cm^2 sec Å, the other in August 1962[2] revealed that the line was weaker and much more deeply reversed with an effective intensity of only 1.6 ergs/cm^2 sec Å. In view of this rapid fall off during the period of decreasing solar activity it is most urgent that a similar measurement be performed very soon before we depart too far from solar minimum. Until and unless such an experiment is performed all of the data obtained during the past two years relating to absolute intensities of airglow Lyman α must be interpreted with reservations and probably give only lower limits to the hydrogen abundance when the solar intensity during 1962 is used in the analysis.

Similarly there is just one measurement reported from NRL of the profile of solar Lyman β.[2] In 1962 it was a deeply reversed line with a central intensity of 7.5×10^{-2} ergs/cm^2 sec Å.

III. ABSORPTION MEASUREMENTS

One single measurement has been made giving the amount of hydrogen in the upper atmosphere from an observation of the equivalent width of the telluric absorption line and its variation with altitude.[1] This, performed in July 1959 by Purcell and Tousey during the same flight which gave us the solar intensity at that time, revealed that during solar maximum in daytime there were $3 \pm 1.5 \times 10^{12}$ atoms of hydrogen per cm^2 column above 120 km.[3]

IV. LYMAN α AIRGLOW

The bulk of the information relating to the hydrogen distribution has derived from some seventeen experiments which have been carried out by various people since 1957 in attempts to observe the Lyman α airglow from rockets and satellites. Results from several of these flights are as yet unavailable and only one satellite experiment has been even a partial success.[4] Unfortunately also for the investigation of a phenomenon under strong solar control with very probably a severe dependence on solar activity and local time the experiments so far performed have tended to be sporadic and unrelated to other experiments. This is partly owing to the difficulty of organizing a series of rocket launchings spaced over a relatively short period of time such as would be required to give a clear picture of the dependence of the Lyman α airglow intensity on the solar zenith angle (or angle from the diurnal atmospheric bulge). It has also been a consequence of the tendency to couple Lyman α observations with other unrelated experiments in the same rocket or satellite payloads so that as a result the mission is rarely one to optimize conditions for attacking the rather specialized requirements of the hydrogen problem. Thus, whereas Lyman α observations have fairly well settled the questions concerning the origin of the nightglow in favor of scattering by terrestrial exospheric hydrogen (at least during solar minimum), and given somewhat crude indications of large diurnal and solar cycle effects, these observations are far from giving a clear quantitative picture of the details in the vertical distribution, the dependence on the solar zenith angle (the diurnal variation) or the changes during the solar cycle.

The Lyman α nightglow was first observed with NO ionization chambers from an Aerobee flown by NRL in 1957.[5] At that time, with

the sun 134° from the zenith the overhead intensity at 120 km was 3 kR. There was a minimum in the anti solar direction and there was a slow 25% increase in brightness as the photometer scanned toward the horizon.

At the 1959 solar Lyman α intensity some 2×10^{12} atoms/cm^2 would have been needed to produce all of this glow by direct scattering. It is now clear that the quantity of interplanetary neutral hydrogen falls far below this. It has been proposed that single scattering is responsible but that the hydrogen is terrestrial in origin swept into a geocoma behind the earth some 15 earth radii by the solar wind.[6] Quantitatively this mechanism has always seemed inadequate.[7] Furthermore in December, 1964 Barth and Fastie,[8] using instruments with high spatial resolution, were unable to detect any sharp changes in intensity as they scanned through the anti-solar direction from a point close to the anti-solar point. Indeed the variation in intensity as the photometer axis swept through the anti-solar direction to the horizon and down across the earth showed the same slowly changing pattern always found by wide angle photometers. No appreciable contribution from a geocoma could have come from closer than some twenty earth radii. The small horizon brightening still evident indicates that the principal contribution to the scattered Lyman α is geocoronal even at the anti-solar point and that the nocturnal hydrogen geocorona must have had appreciable optical thickness to transport radiation so deep into the shadow by multiple scattering. It should be noted, however, that there is little question that the telluric hydrogen is quite thick optically both on the day and night sides of the earth during solar minimum when the exospheric temperature is very low. Thus there is little reason to doubt the effectiveness of radiative transport in the geocorona during the present epoch. Furthermore the direct scattered

radiation from any presumed geocoma would suffer multiple scattering in the geocorona and the sharp shadow boundary would be washed out. Nevertheless if the geocoma had been able to produce 2 to 3 kR of direct scattered Lyman α in 1959 it would contribute about 1 kR now and would be seen to cause a distinct and deep valley in the intensity in the anti-solar direction.

The optical thickness for resonant scattering is defined as

$$\tau = \sigma_o \int n(H)dz$$

where σ_o is the cross section for scattering at the center of the resonance line here presumed to have a Doppler shape. In the case of hydrogen at about 1000° σ_o is of the order of 1.5×10^{-12} cm^2 so that the optical thickness above 120 km of the hydrogen observed during the daytime in 1959 was only about 0.5. The solution of the radiative transport problem for geocoronal hydrogen by Thomas[9] showed that this was insufficient for multiple scattering to carry enough photons around to the night side and produce the zenith brightness of 3 kR observed at 134° solar zenith angle. An optical thickness of about 3 was required. Thus to accept the daytime absorption measurement, the solar line intensity measurement, the nightglow measurement and ascribe the radiation observed to geocoronal scattering, would require that there exist a large diurnal effect with much more hydrogen on the cool night side of the earth than on the warm sunlit hemisphere.[10]

As F. S. Johnson had pointed out[11] this sort of behavior was to be expected for hydrogen escaping from the base of the exosphere at a rate not insignificant in comparison with the upward flux which

can be provided by diffusion in the thermosphere. The large diffusive flow means that hydrogen is far from a diffusive equillibrium. The decrease in escape flux which follows a reduction in exospheric temperature thus permits a build up of hydrogen below the base of the exosphere and the hydrogen content of the atmosphere should tend to increase with decreasing exospheric temperature.

A quantitative treatment of this effect was given first by Mange[12] who solved the diffusion equation subject to flow. His calculation was followed by the more detailed treatments of Bates and Patterson[3] and of Kockarts and Nicolet.[13] From these it was apparent that the dependence of the hydrogen content on exospheric temperature for an atmosphere in a steady state with the exospheric temperature a constant everywhere on the critical surface was strong enough to produce the effect required. However, it is still now known on a theoretical basis how close the approach to a steady state will be in the real atmosphere where the oscillation between extremes in temperature occurs within a period of the order of twenty four hours. It is particularly in the lower thermosphere that the adjustment is the slowest and the density there limits the density at higher altitudes. Furthermore, there is also a tendency for flow to occur between points on the critical surface if density and thermal gradients exist. This is a result of an umbalance among the atoms traversing the exosphere on elliptical orbits. In the case of hydrogen the two types of gradients have opposite signs to that the nocturnal bulge will certainly not be eliminated by flow. The problem has been to determine how large an asymmetry can be maintained against lateral flow of this type and also to assess the effect of the flow on the distribution below the base of the exosphere. A partial solution to this problem has been obtained by McAfee[14] and will be discussed in section VII.

During the past few years further experiments on the Lyman airglow have brought into evidence the existence of the diurnal variation in abundance and a general increase in the hydrogen content of the atmosphere during a period of decreasing exospheric temperature. These experiments have involved measuring the dependence on altitude of the Lyman α glow during the daytime and during (exospheric) twilight as well as late at night.

The theory of resonance scattering of solar Lyman α to produce the Lyman α airglow has been developed by Thomas[9] and Donahue[15] and recently also by Kurt.[16] In the daytime solar photons traversing the terrestrial hydrogen are scattered from the solar beam isotropically. If the optical thickness of the hydrogen is large enough there is an appreciable chance that these photons will be rescattered several times before they escape outward or finally penetrate below 100 km where they finally are absorbed by O_2. The optical depth scale in which it is simplest to discuss the transfer problem is a highly non linear function of distance. It begins at infinity and terminates near 100 km where true absorption sets in. Roughly half of the optical depth is concentrated between the 100 and 120 km levels where the hydrogen density varies rapidly. On the other hand at high altitudes the hydrogen density according to theory varies so slowly that large distances must be traversed before there is an appreciable change in the optical depth scale. For example if the exospheric temperature is 850° 46% of the hydrogen lies between 100 and 200 km, 60% between 100 and 500 km, 73% between 100 and 1000 km and 87% between 100 and 2000 km.

As long as the total optical thickness is less than unity the dayglow brightness at the zenith will decrease steadily with altitude above the base of the absorption region. As the optical thickness

increases, however, so many incident photons are scattered at high altitude whence it is difficult for them to penetrate deep in the atmosphere that a maximum develops about half way through the medium. Because of the peculiar nature of the hydrogen distribution this maximum will never be found very high in the atmosphere and it will always be difficult to separate the part of the increase in brightness between 90 km and 150 km which is caused by multiple resonance scattering and the part caused by a decrease in true absorption. Curves showing the dependence of zenith brightness on the residual optical thickness above for solar zenith angles of 60° and 75° are shown in Figs. 1-3. The 60° case is transformed to a scale of actual altitude for exospheric temperatures of 1000° and 850° in Figs. 4 and 5. It is clearly necessary to probe far above 1000 km before an appreciable drop in dayglow brightness is to be anticipated.

So far there have been three dayglow flights at 60° solar zenith angle. These were carried out by Fastie in 1962[17] when the Lyman α dayglow proper was first observed, in 1963[17] and to high altitude (1200 km) in late 1964.[18] In all cases a scanning uv spectrophotometer was used for spectral resolution and the detector was a photomultiplier. The experimental data are plotted in Figs. 3 and 4. They show the expected rapid increase below 120 km and the very flat profile above. The first two flights did not go high enought to permit any deductions from the altitude profiles. The intensities correspond to those for optical thicknesses of 1 and 3.3 above 100 km in 1962 and 1963. In the third flight the altitude profile shows a very slow decrease in intensity (1.3%) between 300 km and 1000 km. This profile corresponds to that expected if the optical depth were 7 and the distribution were that calculated by Kockarts and Nicolet for an exospheric temperature of 850° if the hydrogen

density at 100 km is taken to be 2×10^7 per cm^3. However, the intensity measured by Fastie (1.1 kR) is far too low to be consistent with such an abundance unless the effective solar flux had dropped to about 5% of its 1962 value.

When the sun gets very low the long slant path accentuates the deposition of excitation at high altitude (Fig. 5) so that the increase in brightness with increasing altitude below 150 km grows less abrupt. This becomes particularly dramatic after sunset (Fig. 6) when only the upper regions of the atmosphere are sunlit. The hydrogen below the shadow surface serves by scattering to attenuate the photons coming from the sunlit region. Thus the overhead brightness increases slowly up to some 200 km as the detector penetrates the attenuating hydrogen layer. The rate of increase of brightness with altitude is a sensitive measure of the hydrogen abundance below the shadow. The twofold increase between 120 km and 200 km observed by Fastie[17] in 1962 with the sun 30° below the horizon (Fig. 7) is unambiguous evidence for the existence of an optical thickness of unity between these two levels and hence for a total optical depth of the order of 3 (18×10^{12} atoms/cm^2) above 120 km. Combined with Fastie's observation of an optical thickness of 0.5 (above 120 km) twelve hours before with the sun 30° above the horizon this constitutes a clear indication of the suspected diurnal variation. The ratio of intensities 3.6 kR at night to 12 kR in the day gives an even larger effect - from $\tau = 0.5$ to $\tau = 6$.

There has been a group of three twilight observations obtained by the group at the Shternberg Astrophysical Observatory working with V.I. Kurt in 1963.[19-22] All of these show the expected slow increase in intensity below 200 km (Fig. 7).

Similarly a flight by Blamont[23] just at sunset in 1964 gave the same sort of result. The intensity (3 kR) indicated an optical depth of 3 above 100 km.

At night excitation is entirely by multiple scattering and the variation of brightness with altitude is similar to that in the daytime. There has been only one high altitude probe this by NRL[24] in 1962. The sun was at a zenith angle of 165°. From the way the difference between the intensity looking up and that looking down decreased from 500 km to 1100 km it can be concluded that the density at 500 km was 9×10^4 per cm^3 and at 100 km was 5×10^4 per cm^3. These would imply a column abundance of 15×10^{12} atoms/cm^2, (an optical thickness 2.5 above 120 km)[25] if they are fitted to a Kockarts and Nicolet model for an exospheric temperature of 1000°. To achieve the fit it is necessary to assume a density of 3×10^7 atoms/cm^3 at 100 km.

Two other experiments have been performed at night recently. One already discussed was in December 1964 with the solar zenith angle 170°. The intensity measured by ionization chamber was 1.35 kR while that measured by spectrophotometer was only about 200 kR. For the 1962 solar intensity these would indicate opacities of 14 and 3 above 100 km. Another pair of observations during an aurora at Fort Churchill by Fastie[26] and by Hoerlin and Peek[27] in February 1965 show that no enhancement or unusual behavior is in evidence during an aurora. The two measurements of brightness are again at variance, however. They are respectively about the same as the pair obtained at White Sands and indicate about the same hydrogen abundance. Once again the measurement by Fastie is very low.

All of the zenithal intensities so far reported from 120 km are plotted in Fig. 8 at their appropriate solar zenith angles. Since

only the 1957 NRL result was obtained before 1962 it is plotted twice, once reduced by a factor of 3, to compare it with the theoretical curves which are based on the solar intensity of 1.6 ergs/cm^2 sec Å measured in 1962. These theoretical predictions are based on the radiative transfer calculations for opacities measured from 100 km ranging from 1 to 12. If the solar intensity continued to diminish between 1962 and 1965 the abundances would be even higher than indicated particularly in 1964 and 1965. In view of this element of uncertainty and the great disparity among absolute intensities obtained with different instruments even during the same experiment no confidence in quantitative conclusions would be warranted. It appears that the daytime abundance has increased from about 6 x 10^{12} atoms/cm^2 above 100 km in 1959 to perhaps 40 x 10^{12} atoms/cm^2 in late 1964 while the night time abundance has increased from roughly 30 x 10^{12} atoms/cm^2 to more than 85 x 10^{12} atoms/cm^2 during the same period. The solar minimum values, as already noted might be much higher.

In Table 1 the information available on hydrogen abundance from Lyman α studies is collected. It is indicated whether the abundance listed is deduced from intensity, vertical profile or absorption.

In view of the strong dependence of brightness on solar zenith angle indicated by the theory it is evident that a series of experiments at a number of solar zenith angles rom 40° to 160° taken at 30° intervals over a reasonably short period of time if not on one day would help considerably to give a picture of what the hydrogen is doing. At $\tau = 3$ the ratio of intensities for solar zenith angles of 100° and 180° is 8; at $\tau = 6$ it is 5.5; while at $\tau = 12$ it is 4.7. To map out the vertical distribution probes which penetrate much more deeply than Javelins are needed. It is necessary to get at least to 2000 km and

Table 1

Day					Twilight					Night				
Date		ξ	τ_v	I P A	Date		ξ	τ_v	I P A	Date		ξ	τ_v	I P
Aug.	59	60°	1	✓						Mar.	57	135°	9	✓
June	62	60°	1	✓ ✓	June	62	120°	6	✓	June	60	165°	6	✓
May	63	60°	3	✓ ✓				15	✓					
	64	60°	2.3	✓	July	63	85°	1.8	✓ ✓					
Nov.	64	60°	7	✓	Oct.	63	87°	6	✓ ✓	Dec.	64	170°	14	✓
			0.5	✓	Dec.	63	107°	2	✓	Feb.	65	130°	14	✓
June	65	9°	1.7	✓				6	✓					
					Dec.	64	90°	3	✓ ✓					

preferably to two earth radii for an adequate vertical mapping. A great deal could be learned from a system of two small satellites both in circular orbits, one not much higher than 200 km the other at about 7000 km. With three photometers on each satellite, one space oriented (pointed toward the zenith), another earth oriented, and the third looking ahead in the orbital plane the vertical distribution as a function of solar zenith angle could rapidly be plotted. Supplemented by a small number of deep vertical probes, measuring zenith and radir intensities from 100 km to 10,000 km, such experiments should be able to yield valuable information about the hydrogen distribution.

V. BALMER α NIGHTGLOW

Lyman α should be accompanied by H_α radiated from hydrogen atoms which are excited by solar Lyman β . Interpretation of results obtained from H_α studies up to the present is hampered by the sparce information concerning the central intensity of Lyman β . There exists one the one profile obtained by Tousey's group in 1962.

On the basis of a single scattering model for nightglow Lyman only 0.5R of H_α should have paralleled the Lyman α glow in 1959 and it should have had the same spatial distribution.[28] In fact during 1961 the average H_α intensity was 6R for solar elongations between 26° and 113° and 4.2 R between 85° and 170°. Even if Lyman α was three times as intense in 1961 as it was in 1962 this is a factor of about 5 too high.

On the other hand, the optical thickness of hydrogen for Lyman β is 16% of that for Lyman α . Hence if the hydrogen has optical depths ranging up above 5 for Lyman α (above 300 km) the optical depth for Lyman β is large enough to cause appreciable transport to the

night side by multiple scattering.[28] The 1961 results on H_α obtained by Ingham[29] could be accounted for on this model provided the central intensity of Lyman β was indeed a factor of 4 higher in 1961.

More recently Scheglov[30] has reported very detailed results mapping the sky in H_α by observations obtained during very short exposures by using image converters. The dependence of H_α intensity on elongation in the plane of the ecliptic follows that expected for multiple scattering of Lyman β . There are, however, three anomalies in the observations.

The intensities are 8R at 180° elongation and 30R at 90° elongation in the morning. This is a full order of magnitude higher than expected.

There is an apparent strong decrease in H_α brightness with distance from the ecliptic. (It is not clear yet whether this is an artifact of the sequence of solar zenith angles in which the observations were performed.)

There is a build up of H_α toward morning sunrise. This is to be expected if the approach of the hydrogen distribution to a steady state is slow on a scale of six hours.

All H_α intensities reported are surprisingly high. Fishkova[31] has systematically been observing H_α since 1960. Her results are reported in the paper by Krassovsky, Shefov and Vaisberg[32] presented at this meeting. The yearly average H_α intensity rose from about 8R in 1958 to a maximum of 18R in 1962 and 1963. In 1964 it was down to 14R. These intensities are all high on the basis of the 1962 Lyman β flux - the 1962 values in particular by a factor of 15. There is also a seasonal variation of the presumed non galactic H_α . From a January minimum of 6R the brightness rises to a July maximum of 20R.

The observations were made in Georgia at the Abastumai Astrophysical Observatory. Some such seasonal variation can be expected where the maximum solar depression angle varies from 23° in summer to 75° in winter since the multiple scattering source function depends strongly on the solar zenith angle. It is again the absolute brightness which is disturbing. Clearly another measurement of the Lyman β profile is most urgently needed. Observers should also note that care should be taken to report not only solar elongation but solar zenith angles also when describing H_α measurements.

VI EXTRA-TERRESTRIAL LYMAN α

A very interesting and powerful technique introduced by Morton and Purcell[33] of NRL has provided a means of separating the relatively narrow spectral component of Lyman α ascribable to geocoronal scattering from a much broader component which it seems must be extra-terrestrial. This consists of placing an absorption cell in which optically thick atomic hydrogen may periodically be produced in front of a Lyman α detector. This device in 1961 showed that about 0.54 kR - or 15% of the nightglow Lyman α was broad. The source appeared to be uniform over the upward hemisphere. Evidence for such a source[25] also can be found in an overhead excell of Lyman α observed at 1100 km in the high altitude nightglow experiment performed by NRL in 1959. The source of this radiation is in dispute since it might originate in scattering from back streaming hydrogen produced at the turbulent boundary of the solar wind[34] and it might be galactic.[35] If its origin is in the solar system and the solar wind had not changed character drastically in the meanwhile this component should have diminished to 0.18 kR in 1962 and perhaps further by now while the normal nightglow has diminished to 1 to 2 kR depending on solar

depression. If, on the other hand the source is galactic its intensity should not have changed and would remain at 0.54 kR - about 50% of the nightglow intensity. It is most important therefore that these two components be disentangled quantitatively now when the nightglow is weak. For the intensities plotted in Fig. 9 would need to be reduced by a factor of about two if the broad component is still on the order of 0.54 kR. The absorption cell technique should be exploited much more fully than it has been.

Since the broad component will not contribute appreciably to the Lyman α albedo it would be expected that the percentage of albedo in the experiment by Barth and Fastie at White Sands in 1964 would be on the order of 25% if there were 0.54 kR in the broad component. In other words, the albedo should have been about 40% of the 0.8 kR which would constitute the narrow component in the overhead Lyman α . In fact the albedo was 50%, hence the broad component should not have been a major constituent in the incident Lyman α .

VII RECENT THEORETICAL ADVANCES

The current status of theories giving the distribution of hydrogen in the thermosphere and exosphere is being reviewed by F. Johnson and Kockarts at this symposium. It is clear that no Lyman α or H_α experiments so far reported can yield details about the exospheric distribution. The experiment being carried out by Mange on OGO 1 is in principle capable of yielding such data. However, his results are not yet in a proper state of reduction to be reported. In any event the steady state theories are probably far from giving a good approximation to the true hydrogen distribution below some 10,000 km. This is in part because of the time required for the lower thermosphere to adjust to a changing escape flux. It is also a consequence of the

fact that where density and temperature gradients exist on the critical surface the flux of reentering and outgoing atoms in the ballistic orbit component will not be balanced. Crude calculations on this effect have already been published.[36,37] Recently McAfee has carried out a detailed calculation using spherical geometry in which he has permitted the temperature at the exospheric base to vary and the altitude of the base also to vary with the temperature. In one case he has assumed that the local density at a point on the exospheric base is given by the steady state theory appropriate to the local temperature. This produces a large density gradient opposite in sense to the temperature gradient. By following the ballistic orbits he then computes the flux in and flux out at every point for hydrogen and also for other gases. The flows resulting are very large for hydrogen and because density and temperature gradients have the same sign, for helium. Results for the temperature ranges 2100°-1500°, 1500°-1100°, 1100°-700° are shown in Figs. 9-11. In Tables 2-4 the fluxes resulting from lateral flow are compared to escape fluxes and also to the maximum flow that diffusion will support. (When the flow is larger than the maximum solution of the diffusion equation gives a vanishing density at some point below the base of the exosphere). Since the time constant for the flow is very low these densities cannot be maintained at the base of the exosphere. McAfee has also calculated the density distribution which would be required for a given temperature variation to produce a condition of balance everywhere with no flux due to lateral flow. The results are shown in Figs. 12-14. It should be noted that these are the base of the exosphere. The maximum and minimum altitudes are noted on the figures. The density variation given by the steady state theory is also shown. Since the hydrogen density at the temperature maximum is higher than the steady

state density and this is the density which balances escape flux and diffusive flow it is clear that the actual density variation must lie between these two extremes. In the zero flow distribution the escape flux is too high at the point of temperature maximum and too low at temperature minimum. Thus escape and diffusive flow will surely cut down the density at the temperature maximum and build it up at the minimum. It should be noted that the effect may be large for helium. Densities may differ by as much as 50% at the exospheric base than those computed for the steady state. On the other hand, flow will never wipe out or even seriously reduce the diurnal effect in hydrogen at least above the base of the exosphere.

McAfee has also calculated vertical density distributions for these models. Results are shown in Figs. 15 and 16 for Hydrogen and Helium. The diurnal variation in hydrogen can be seen to produce important effects out to 5000 km. Eventually of course the distribution must tend asyntotically to a spherically symmetric one.

The horizontal flow can produce large scale winds above the base of the exosphere. For example, in the extreme case of where the diurnal temperature oscillation is from 1500° to 1000° and the densities are as given by the steady state thermospheric theories the average helium horizontal velocity above the terminator is 50 m/sec and the average hydrogen velocity 540 m/sec. Wind velocities increase with altitude, being below the average near the critical surface and then building up as the altitude increases. How large the velocities would be in the real case is not known.

Obviously the phenomenon of lateral flow adds another element of complexity to the time dependent problem since the entire vertical profile above any one point influences and is in turn influenced by every other part of the atmosphere is an important way.

Two similar calculations performed recently are designed to assess the effect of assuming a sharp surface of discontinuity for the velocity distribution function at the base of the exosphere.[38,39] Lifschitz and Singer have replaced the surface of discontinuity by a layer. They feed atoms in the Maxwell-Boltzmann distribution from below, and follow them by Monte-Carlo techniques until they reach the base of the exosphere. There they permit those above escape velocity to pass on and be lost but require that all others be reflected. The result is a decrease in density with decreasing slope through the boundary layer and a strong anisotropic cooling. Results obtained by Lifschitz and Singer for the density at the base are

	1000°	2000°
for a sharp base	8×10^4	4.5×10^3 cm^{-3}
for a layer	3×10^4	1.5×10^3 cm^{-3}

For the effective temperature they find

Sharp Base	Layer
2000°	1400°
1500°	1100°
1000°	800°

The result is a reduction in effusion velocity by a factor of three and the prediction that the atmosphere, for a given hydrogen density at 100 km, retains much more hydrogen than previously was believed, particularly during solar minimum. The predictions for the hydrogen column abundance between 120 km and infinity are in atoms/cm^2

	1000°	1500°	2000°
Sharp Base	21×10^{12}	7.2×10^{12}	5.7×10^{12}
Layer	40×10^{12}	12.5×10^{12}	7.5×10^{12}

where the normalization is to 3×10^7 atoms/cm^3 at 100 km.

The experimental results indicate (as lower limits)

700° (night)	850° (day)	1500° (night)	2000° (day)
60×10^{12}	24×10^{12}	18×10^{12}	$2\text{-}5 \times 10^{12}$

It should be noted that taking into account the effects of lateral flow actual night time densities should be lower than the steady state calculated values for the same temperature and daytime densities higher.

Acknowledgement

This work was supported in part by the National Science Foundation, Atmospheric Sciences Section, under Grant (G-21999) and the National Aeronautics and Space Administration under Contract Nasr 179.

Table 2. Pertinent fluxes for 700-1000° temperature variation.

Constituent	Angle	Lateral flux	Escape flux	Max.Diff.flux
H	0	2.29×10^{8}	0.55×10^{7}	8.9×10^{7}
	30	1.11×10^{8}	0.69×10^{7}	8.9×10^{7}
	60	-1.14×10^{8}	1.20×10^{7}	8.9×10^{7}
	90	-1.82×10^{8}	2.12×10^{7}	8.9×10^{7}
	120	0.24×10^{8}	3.11×10^{7}	8.9×10^{7}
	150	3.44×10^{8}	3.63×10^{7}	8.9×10^{7}
	180	4.97×10^{8}	3.73×10^{7}	8.9×10^{7}
He	0	1.56×10^{8}	4.26×10^{-6}	5.4×10^{8}
	30	1.36×10^{8}	1.29×10^{-5}	5.4×10^{8}
	60	0.78×10^{8}	2.00×10^{-4}	5.4×10^{8}
	90	-0.10×10^{8}	4.64×10^{-3}	5.3×10^{8}
	120	-0.86×10^{8}	6.31×10^{-2}	5.3×10^{8}
	150	-1.22×10^{8}	3.26×10^{-1}	5.3×10^{8}
	180	-1.27×10^{8}	5.65×10^{-1}	5.3×10^{8}
O	0	5.12×10^{7}	-	1.3×10^{11}
	30	4.44×10^{7}	-	1.3×10^{11}
	60	2.38×10^{7}	-	1.3×10^{11}
	90	-0.40×10^{7}	-	1.2×10^{11}
	120	-2.69×10^{7}	-	1.2×10^{11}
	150	-3.58×10^{7}	-	1.2×10^{11}
	180	-3.65×10^{7}	-	1.2×10^{11}
N_2	0	5.57×10^{5}	-	2.5×10^{10}
	30	4.80×10^{5}	-	2.5×10^{10}
	60	2.53×10^{5}	-	2.4×10^{10}
	90	-0.52×10^{5}	-	2.3×10^{10}
	120	-3.00×10^{5}	-	2.2×10^{10}
	150	-3.88×10^{5}	-	2.1×10^{10}
	180	-3.90×10^{5}	-	2.1×10^{10}
O_2	0	8.10×10^{3}	-	3.5×10^{8}
	30	7.00×10^{3}	-	3.5×10^{8}
	60	3.84×10^{3}	-	3.4×10^{8}
	90	-0.81×10^{3}	-	3.2×10^{8}
	120	-4.52×10^{3}	-	3.1×10^{8}
	150	-5.68×10^{3}	-	3.0×10^{8}
	180	-5.71×10^{3}	-	3.0×10^{8}

Table 3. Pertinent fluxes for 1000-1500^{o} temperature variation.

Constituent	Angle	Lateral flux	Excape flux	Max.Diff.flux
	0	-3.34×10^{8}	3.73×10^{7}	8.9×10^{7}
	30	-3.59×10^{8}	4.39×10^{7}	8.9×10^{7}
	60	-3.38×10^{8}	6.28×10^{7}	8.9×10^{7}
H	90	-1.23×10^{8}	8.45×10^{7}	8.8×10^{7}
	120	2.77×10^{8}	8.86×10^{7}	8.8×10^{7}
	150	6.67×10^{8}	7.13×10^{7}	8.8×10^{7}
	180	8.28×10^{8}	5.92×10^{7}	8.8×10^{7}
	0	3.82×10^{8}	5.65×10^{-1}	5.3×10^{8}
	30	3.34×10^{8}	1.38×10^{0}	5.3×10^{8}
	60	1.91×10^{8}	1.20×10^{1}	5.3×10^{8}
He	90	-0.30×10^{8}	1.34×10^{2}	5.3×10^{8}
	120	-2.19×10^{8}	9.33×10^{2}	5.3×10^{8}
	150	-2.97×10^{8}	3.07×10^{7}	5.3×10^{8}
	180	-3.07×10^{8}	4.56×10^{3}	5.3×10^{8}
	0	1.07×10^{8}	-	1.2×10^{11}
	30	0.94×10^{8}	-	1.2×10^{11}
	60	0.53×10^{8}	-	1.2×10^{11}
O	90	-0.08×10^{8}	-	1.1×10^{11}
	120	-0.59×10^{8}	-	1.1×10^{11}
	150	-0.78×10^{8}	-	1.1×10^{11}
	180	-0.79×10^{8}	-	1.1×10^{11}
	0	1.16×10^{6}	-	2.1×10^{10}
	30	1.03×10^{6}	-	2.1×10^{10}
	60	0.57×10^{6}	-	2.0×10^{10}
N_2	90	-0.09×10^{6}	-	1.9×10^{10}
	120	-0.64×10^{6}	-	1.9×10^{10}
	150	-0.85×10^{6}	-	1.8×10^{10}
	180	-0.86×10^{6}	-	1.8×10^{10}
	0	1.71×10^{4}	-	3.0×10^{8}
	30	1.50×10^{4}	-	2.9×10^{8}
	60	0.83×10^{4}	-	2.8×10^{8}
O_2	90	-0.13×10^{4}	-	2.7×10^{8}
	120	-0.95×10^{4}	-	2.6×10^{8}
	150	-1.26×10^{4}	-	2.5×10^{8}
	180	-1.28×10^{4}	-	2.5×10^{8}

Table 4. Pertinent fluxes for 1500-2100° temperature variation.

Constituent	Angle	Lateral flux	Escape flux	Max.Diff.flux
	0	-1.52×10^{8}	5.92×10^{7}	8.8×10^{7}
	30	-1.40×10^{8}	6.34×10^{7}	8.8×10^{7}
	60	-0.95×10^{8}	7.31×10^{7}	8.8×10^{7}
H	90	-0.13×10^{8}	8.04×10^{7}	8.8×10^{7}
	120	0.89×10^{8}	7.75×10^{7}	8.8×10^{7}
	150	1.71×10^{8}	6.73×10^{7}	8.8×10^{7}
	180	2.03×10^{8}	6.16×10^{7}	8.8×10^{7}
	0	7.90×10^{8}	4.56×10^{3}	5.3×10^{8}
	30	6.71×10^{8}	7.28×10^{3}	5.3×10^{8}
	60	3.45×10^{8}	2.31×10^{4}	5.3×10^{8}
He	90	-0.63×10^{8}	8.75×10^{4}	5.3×10^{8}
	120	-3.75×10^{8}	2.64×10^{5}	5.3×10^{8}
	150	-5.16×10^{8}	5.27×10^{5}	5.3×10^{8}
	180	-5.46×10^{8}	6.64×10^{5}	5.3×10^{8}
	0	1.54×10^{8}	-	1.1×10^{11}
	30	1.31×10^{8}	-	1.1×10^{11}
	60	0.69×10^{8}	-	1.1×10^{11}
O	90	-0.16×10^{8}	-	1.0×10^{11}
	120	-0.80×10^{8}	-	1.0×10^{11}
	150	-0.99×10^{8}	-	1.0×10^{11}
	180	-0.97×10^{8}	-	1.0×10^{11}
	0	1.60×10^{6}	-	1.8×10^{10}
	30	1.35×10^{6}	-	1.8×10^{10}
	60	0.67×10^{6}	-	1.7×10^{10}
N_2	90	-0.22×10^{6}	-	1.6×10^{10}
	120	-0.79×10^{6}	-	1.6×10^{10}
	150	-0.84×10^{6}	-	1.5×10^{10}
	180	-0.75×10^{6}	-	1.5×10^{10}
	0	2.31×10^{4}	-	2.5×10^{8}
	30	1.94×10^{4}	-	2.4×10^{8}
	60	0.95×10^{4}	-	2.3×10^{8}
O_2	90	-0.35×10^{4}	-	2.2×10^{8}
	120	-1.14×10^{4}	-	2.1×10^{8}
	150	-1.16×10^{4}	-	2.0×10^{8}
	180	-1.00×10^{4}	-	2.0×10^{8}

REFERENCES

1. Purcell, J.D. and Tousey, R., Space Research I, North Holland Publishing Co., Amsterdam, 1960.

2. Tousey, R., Purcell, J. D., Austin, W.E., Garrett, D.L. and Widing, K.G., Space Research IV, Ed. P. Muller, North-Holland, Amsterdam, 1964.

3. Bates, D.R., and Patterson, T.N.L., Planet. Space. Sci. 5, 257, 1961; 5, 328, 1961.

4. Mange, P., Private Communication.

5. Kupperian, J. E., Jr., Byram, E.T., Chubb, T.A., Friedman, H., Ann. Geophys. 14, 329, 1958; Planet. Space Sci. 1, 7, 1959.

6. Brandt, J.C., Astrophys. J. 134, 394, 1961; Nature 195, 894, 1962b.

7. Donahue, T.M., International Dictionary of Geophysics, Ed. Runcorn (to be published).

8. Barth, C. and Fastie, W.G., Private Communication.

9. Thomas, G., J. Geophys. Res. 68, 2639, 1963.

10. Thomas, G. and Donahue, T.M., J. Geophys. Res. 68, 2661, 1963b.

11. Johnson, F. S., Private Communication.

12. Mange, P., presented at IAGA Symposium No. 1, Copenhagen, July 1960; Ann. Geophys. 17, 277, 1961.

13. Kockarts, G. and Nicolet, M., Ann. Geophys. 18, 269, 1962; Ann. Geophys. 19, 1963.

14. McAfee, J., Doctoral Thesis, University of Pittsburgh, 1965.

15. Donahue, T.M. and Fastie, W.G., Proc. 4th Intern. Space Sci. Symp., Warsaw, 1963, North Holland Pub. Co.-Amsterdam.

16. Kaplan, S.A., Katyushina, V.V., and Kurt, V. G., 5th International Space Science Symposium and Cospar Meeting, Florence, Italy, May, 1964.

17. Fastie, W. G., Crosswhite, H.M. and Heath, D.F., J. Geophys. Res. 69, 4129, 1964.

18. Fastie, W.G., Private Communication.

19. Babichenko, S.I., Karpinski, I.P. and others, Cosmic Research, Volume III, 1965 No. 2, pp. 237-243.

20. Katyushina, V.V., Kurt, V.G., Cosmic Research, Volume III, 1965 No. 2 pp. 243-247.

21. Kaplan, S.A., Kurt, V.G., Cosmic Research, Volume III, 1965 No. 2, pp. 251-256.

22. Kaplan, S.A., Kurt, V.G., Cosmic Research, Volume III, 1965 No. 2, pp. 256-261.

23. Blamont, J.E., Private Communication.

24. Chubb, T.A., Friedman, H., Kreplin, R.W. and Mange, P., Mem. Soc. Roy. Sci. Liege, 4, 437, 1961.

25. Donahue, T.M., J. Geophys. Res. 69, 1301, 1964.

26. Fastie, W.G., Private Communication.

27. Hoerlin, H. and Peek, M., Private Communication.

28. Donahue, T.M., Planet. Space Sci. 12, 149, 1964.

29. Ingham, M.F., Mon. Not. Roy. Astr. Soc. 124, 523, 1963.

30. Shcheglov, P.V., Astronomical J. 41, 371, 1964; Soviet Astronomy 8, 289, 1964.

31. Fishkova, L.M., Aurorae and Airglow, IGY Program, Sec. IV, No. 10, ed. V.I. Krassovsky, Moscow, 1963.

32. Krassovsky, V.I., Shefov, N.N. and Vaisberg, O.L. These Proceedings, page

33. Morton, D.C. and Purcell, J.D., Planet. Space Sci. 9, 455, 1962.

34. Patterson, T.N.L., Johnson, F.S., and Hanson, W.B., Planet. Space Sci. 11, 767, 1963.

35. Brandt, J.C., Planet. Space Sci. 12, 650, 1964.

36. Hanson, W.B. and Patterson, T.N.L., Planet. Space Sci. 11, 1035, 1963.

37. Donahue, T.M. and McAfee, J.R., Planet. Space Sci. 12, 1045, 1964.

38. Lifschiz and Singer, S.F., to be published 1965.

39. Lew, S. and Venkateswaran, S.V., to be published 1965.

FIGURE CAPTIONS

Fig. 1 Intensity from the zenith as a function of optical depth from the top of the medium for solar zenith angle of 60°. Altitude in km is indicated where the level $O = \tau_v$ is at 100 km.

Fig. 2 Intensity from the zenith as a function of optical depth from the top of the medium for solar zenith angle of 75°.

Fig. 3 Excitation rate $j(\tau)$ of hydrogen atoms as a function of optical thickness measured from the top of the medium. The factor $(\pi F_o)_\nu \Delta\nu_D \sqrt{\pi}$ was 33.3×10^9 photons/cm^2 sec in 1959 and 11.1×10^9 in 1962. The parameter is the solar zenith angle.

Fig. 4 Intensity in kR divided by $A = (\pi F_o)\ \Delta\nu_D \sqrt{\pi}$ (or 11.1 kR in 1962) as a function of altitude in the dayglow for a solar zenith angle of 60°. Experimental data obtained by Fastie is shown. The lower set of points were obtained in June 1962, the upper set in May 1963.

Fig. 5 Predicted overhead intensity of Lyman α dayglow brightness for an 850° exospheric temperature and various optical thickness measured from 100 km. $\tau = 1$ for this distribution corresponds to a density of 2.3×10^6 per cm^3 at 100 km.

Fig. 6 Excitation rate $j(\tau)$ of hydrogen atoms as a function of optical thickness measured from the top of the medium. The factor $(\pi F_o)\ \Delta\nu_D \sqrt{\pi}$ was 33.3×10^9 photons/cm^2 sec in 1959 and 11.1×10^9 in 1962. The parameter is the solar zenith angle. Altitudes are indicated where the vertical thickness is 9 from 100 km.

Fig. 7 Variation with altitude of the overhead intensity in twilight. The theoretical curve is for a solar zenith angle of 120° in solar minimum with $\tau = 3$ above 120 km. Experimental results at 120° refer to (17) and at 107° refer to (16).

Fig. 8 Predicted and observed zenith intensities at 120 km for various optical thicknesses measured above 100 km. These intensities are based on the 1962 solar flux. The 1957 result is plotted at its measured value and also at one third that value to accomodate the threefold decrease in flux from 1959 to 1962. References are B = Barth, Bl = Blamont, F = Fastie, K = Kurt et al, LA = Los Alamos, N = ONR.

Fig. 9 Vertical flux of hydrogen and helium at the base of the exosphere as a function of solar depression angle (or more exactly angle from temperature minimum). A sinusoidal temperature variation from 2100° to 1500° is assumed.

Fig. 10 Vertical flux of hydrogen and helium at the base of the exosphere as a function of solar depression angle (or more exactly angle from temperature minimum). A sinusoidal temperature variation from 1500° to 1000° is assumed.

Fig. 11 Vertical flux of hydrogen and helium at the base of the exosphere as a function of solar depression angle (or more exactly angle from temperature minimum). A sinusoidal temperature variation from 1000° to 700° is assumed.

Fig. 12 Variation in density at the base of the exosphere giving the flux in Fig. 9 and variation needed for no flux due to lateral flow. (Maximum and minimum altitudes for exospheric base are noted.)

Fig. 13 Variation in density at the base of the exosphere giving the flux in Fig. 10 and variation needed for no flux due to lateral flow. (Maximum and minimum altitudes for exospheric base are noted.)

Fig. 14 Variation in density at the base of the exosphere giving the flux in Fig. 11 and variation needed for no flux due to lateral flox. (Maximum and minimum altitudes for exospheric base are noted.)

Fig. 15 Vertical distribution of hydrogen when lateral flow is taking place under the conditions of Figs. 9-11.

Fig. 16 Vertical distribution of helium when lateral flow is taking place under the conditions of Fig. 9-11.

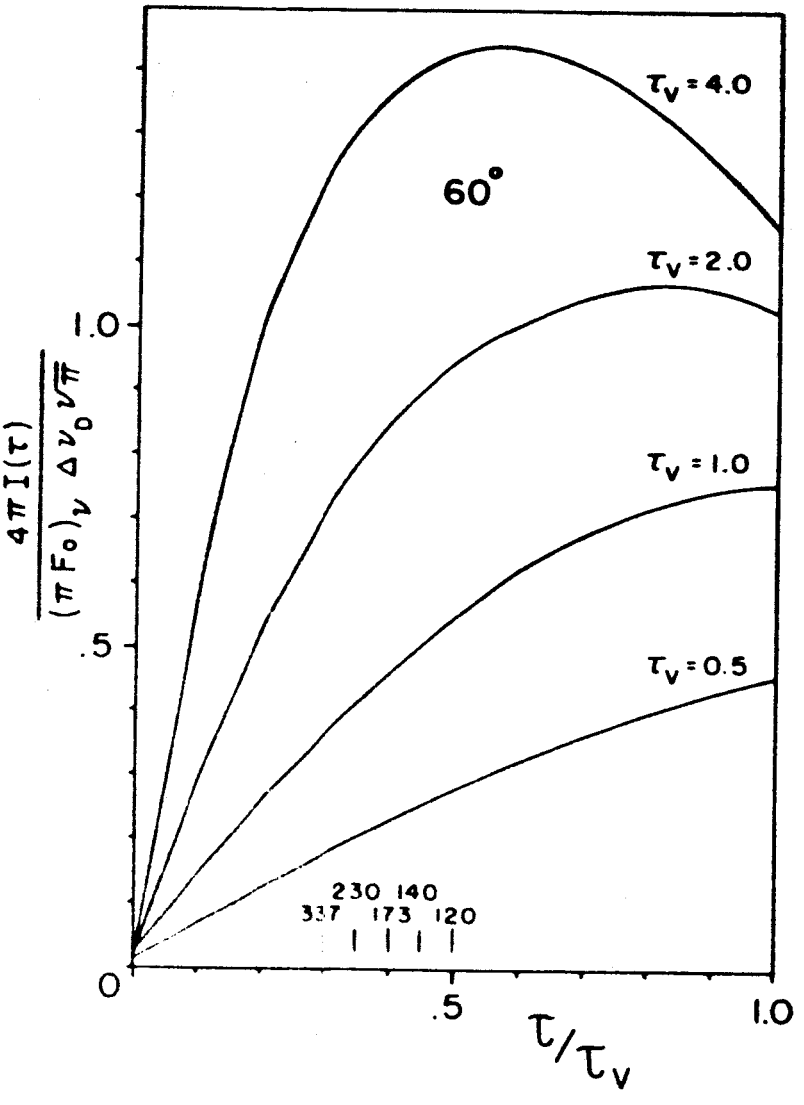
$\tau_V = 4.0$
60°
$\tau_V = 2.0$
$\tau_V = 1.0$
$\tau_V = 0.5$
$\frac{4\pi I(\tau)}{(\pi F_0)_\nu \Delta\nu_0 \sqrt{\pi}}$
1.0
.5
0
230 140
337 173 120
.5
1.0
τ/τ_V

Fig. 1

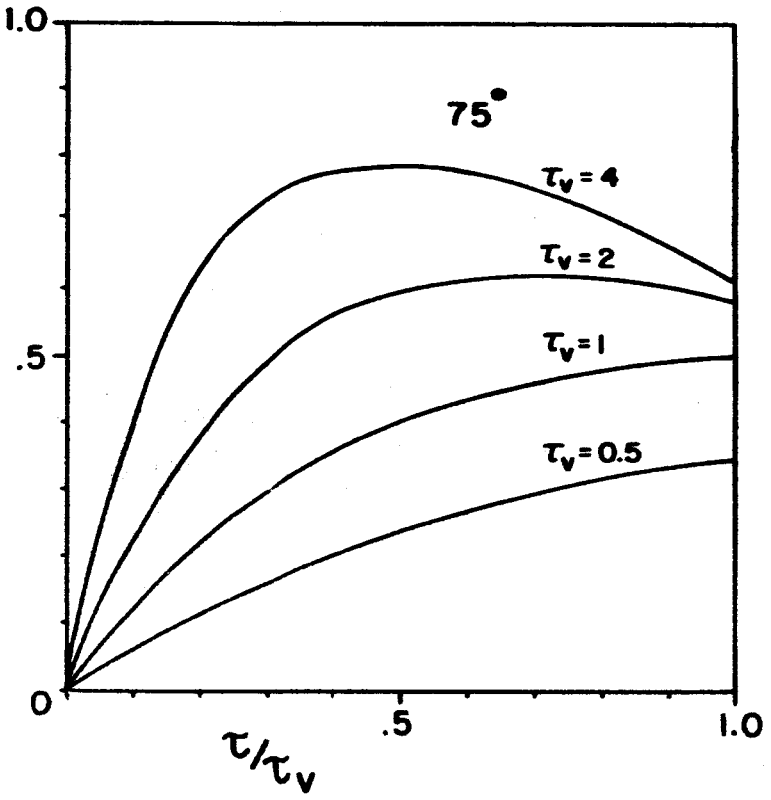

Fig. 2

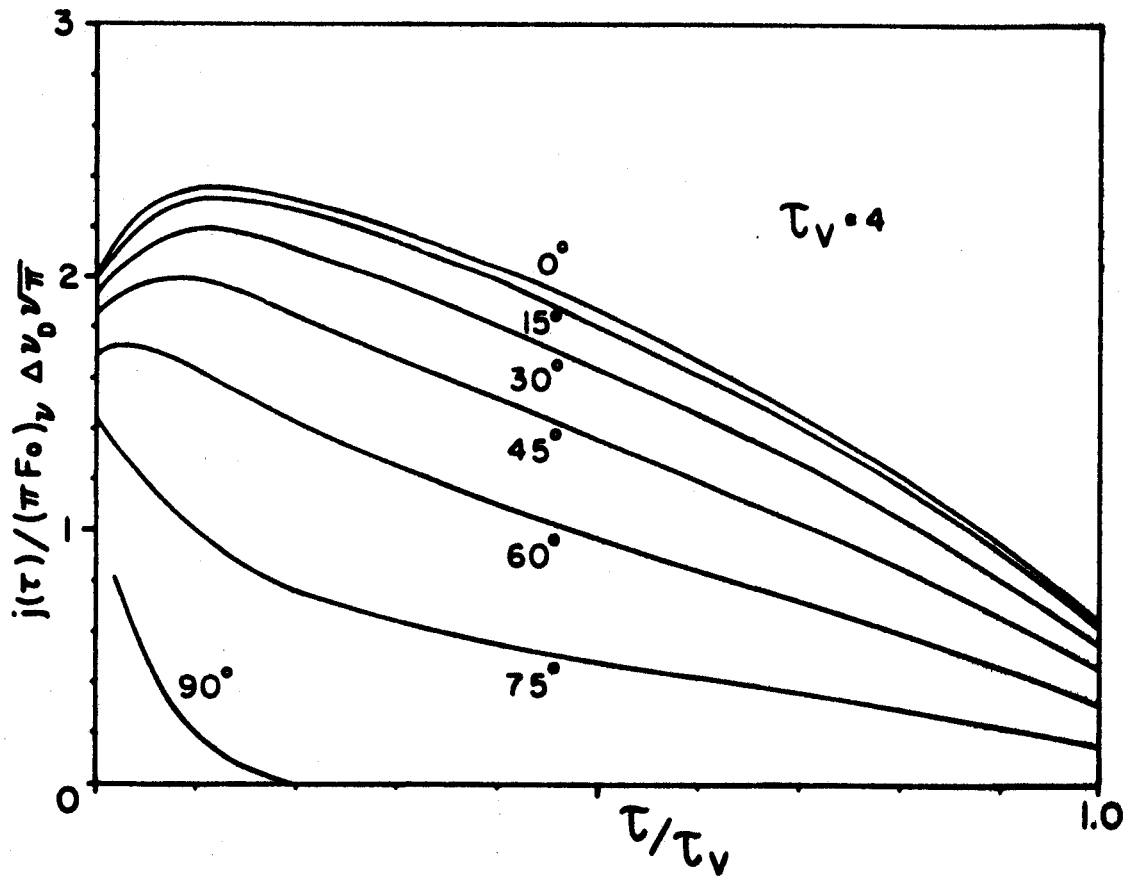
3
2
1
0
$j(\tau)/(\pi F_0)_\nu \Delta\nu_D \sqrt{\pi}$
$\tau_V = 4$
0°
15°
30°
45°
60°
75°
90°
τ/τ_V
1.0

Fig. 3

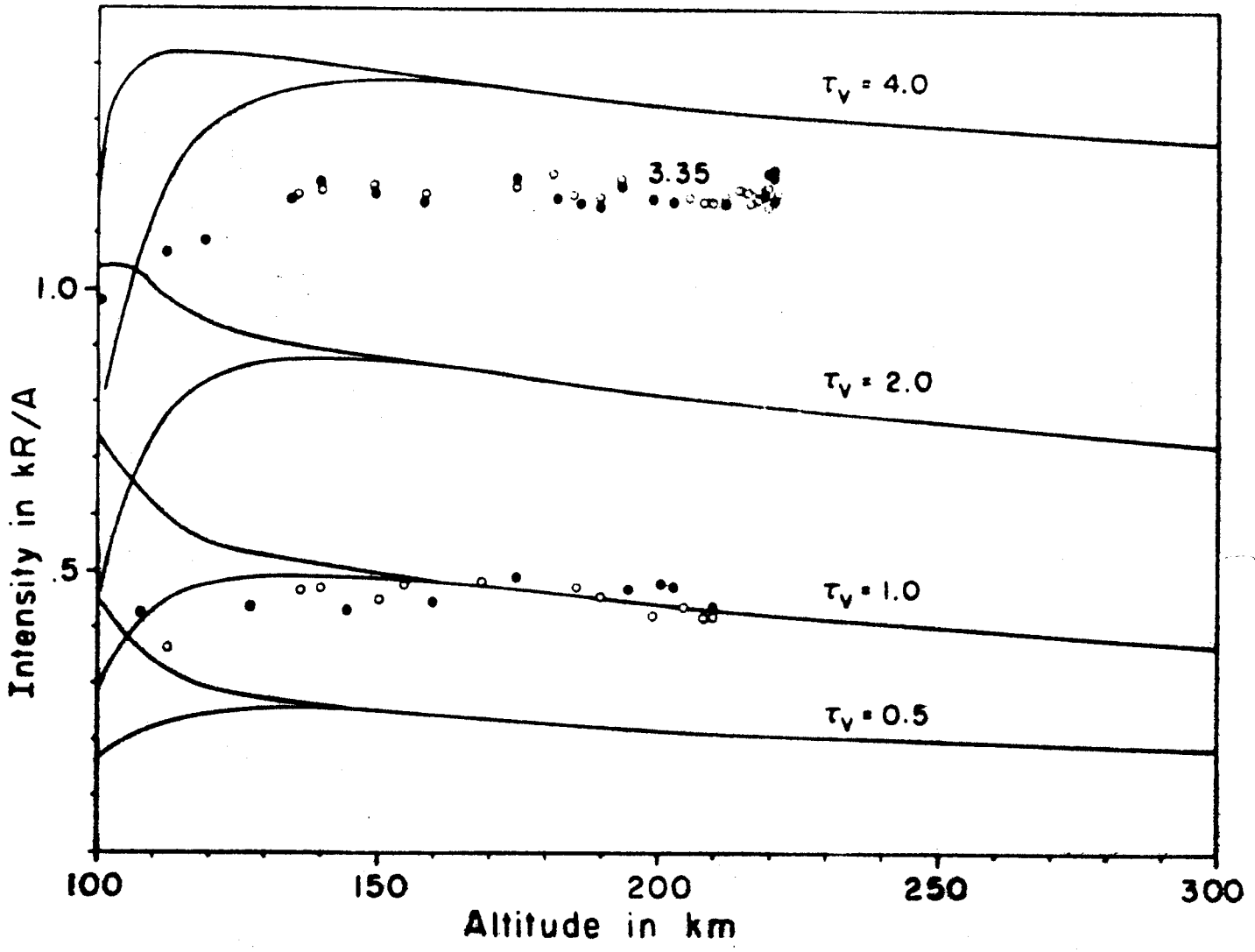
τ_V = 4.0
3.35
τ_V = 2.0
τ_V = 1.0
τ_V = 0.5
1.0
.5
Intensity in kR/A
100
150
200
250
300
Altitude in km

Fig. 4

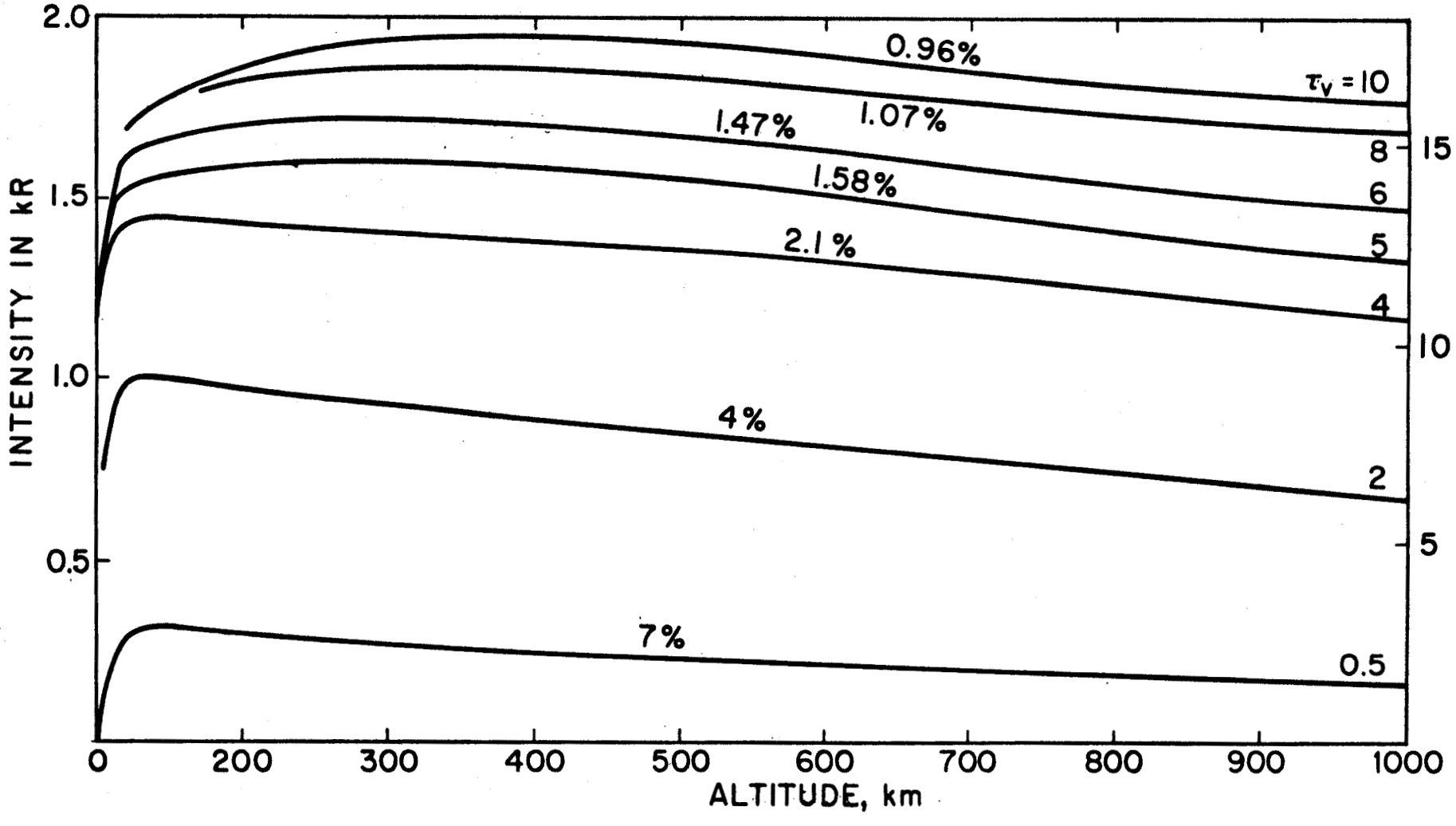
2.0
1.5
1.0
0.5
INTENSITY IN kR
0.96%
1.07%
1.47%
1.58%
2.1%
4%
7%
τ_V = 10
8
6
5
4
2
0.5
15
10
5
0
200
300
400
500
600
700
800
900
1000
ALTITUDE, km

Fig. 5

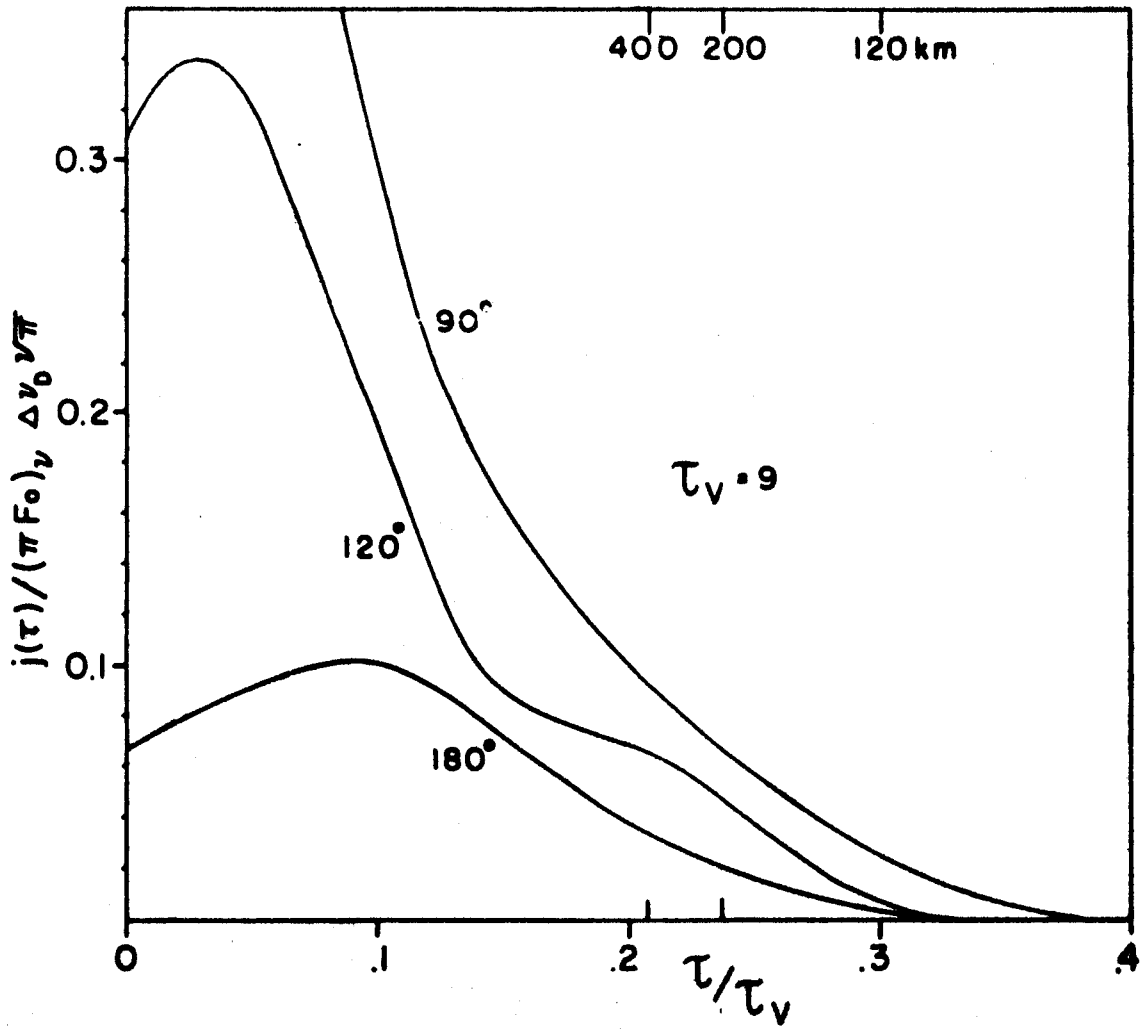
400 200 120 km
0.3
0.2
0.1
$j(\tau)/(\pi F_0)_\nu \Delta\nu_0 \sqrt{\pi}$
90°
120°
180°
$\tau_V = 9$
0
.1
.2
.3
.4
τ/τ_V

Fig. 6

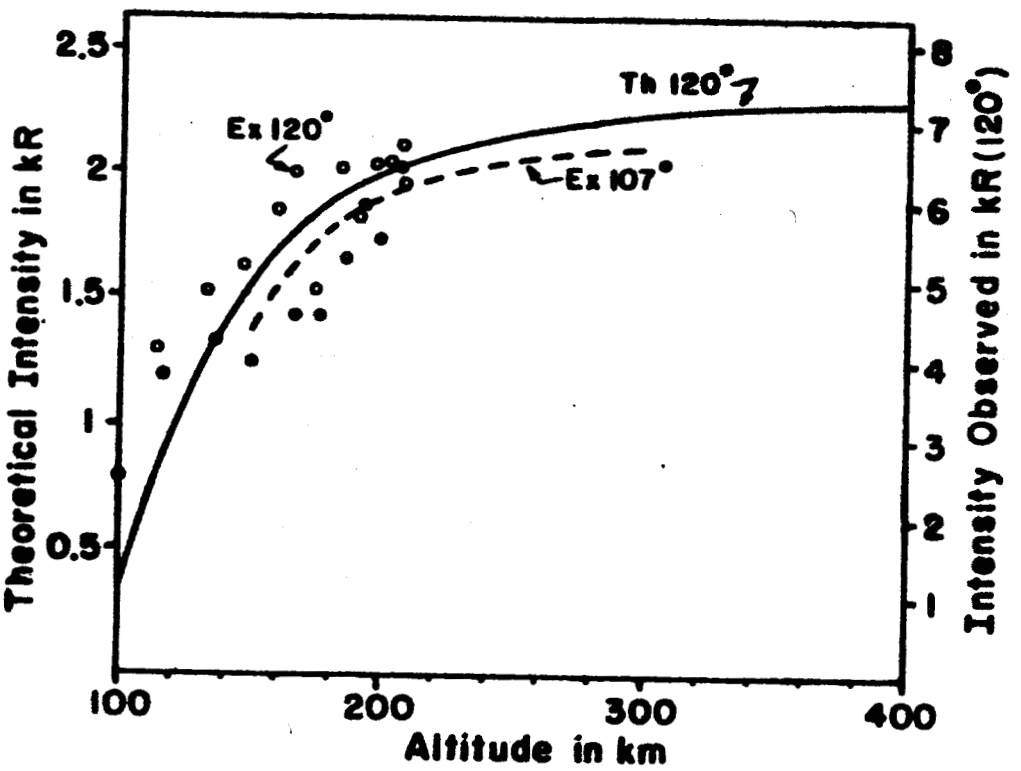
Theoretical Intensity in kR
Intensity Observed in kR(120°)
Altitude in km
Th 120°
Ex 120°
Ex 107°
2.5
2
1.5
1
0.5
8
7
6
5
4
3
2
1
100
200
300
400

Fig. 7

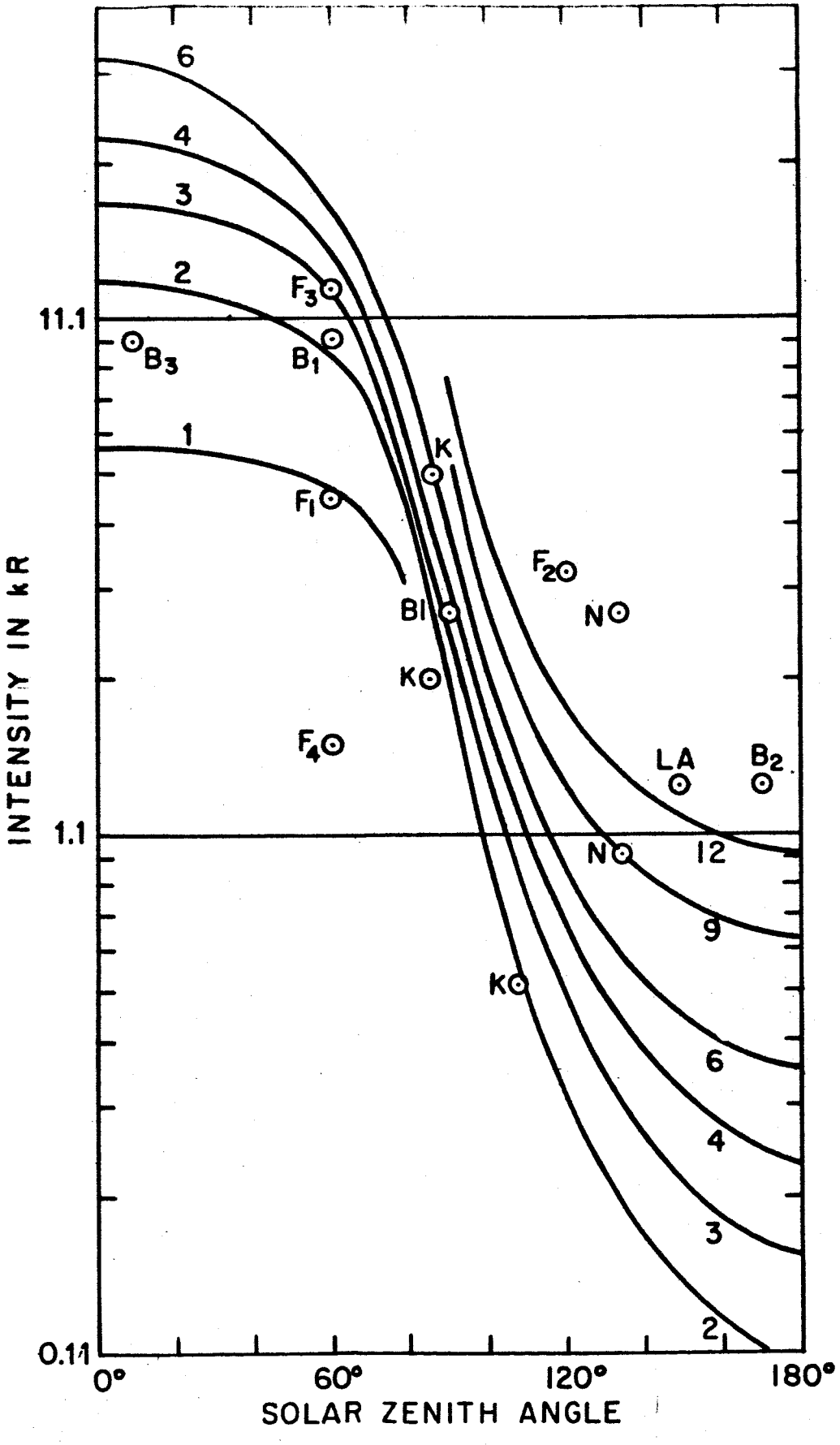
6
4
3
2
1
11.1
1.1
0.11
F_3
B_3
B_1
F_1
K
F_2
N
Bl
K
F_4
LA
B_2
N
12
9
K
6
4
3
2
INTENSITY IN kR
0°
60°
120°
180°
SOLAR ZENITH ANGLE

Fig. 8

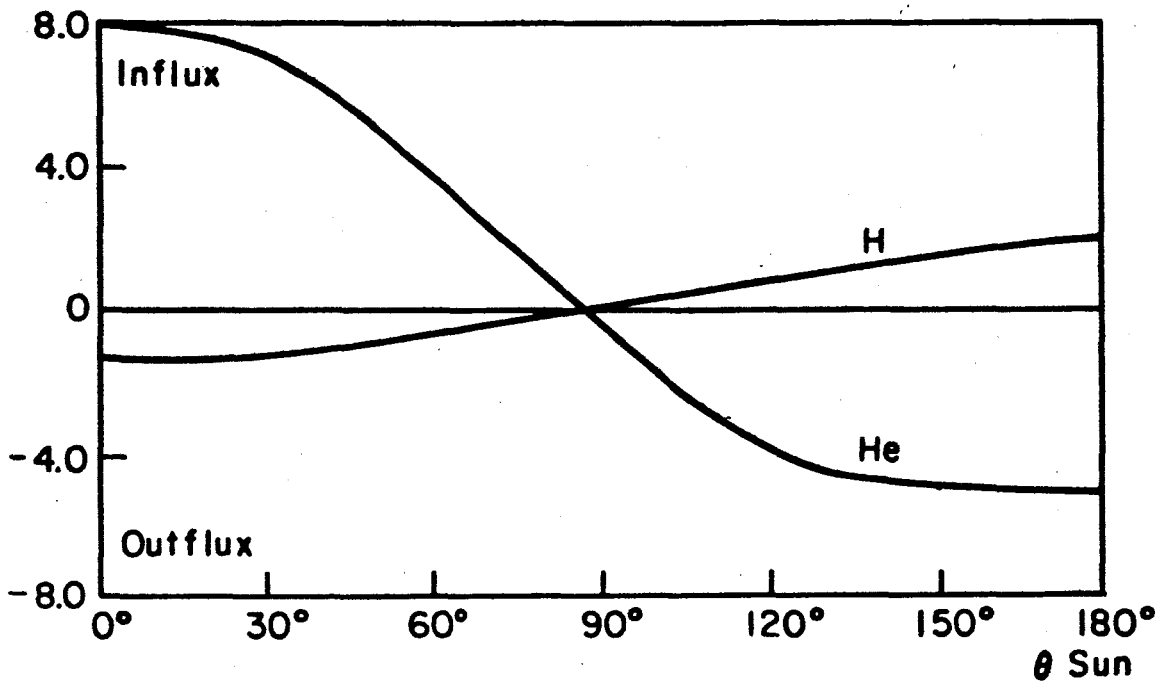

Fig. 9

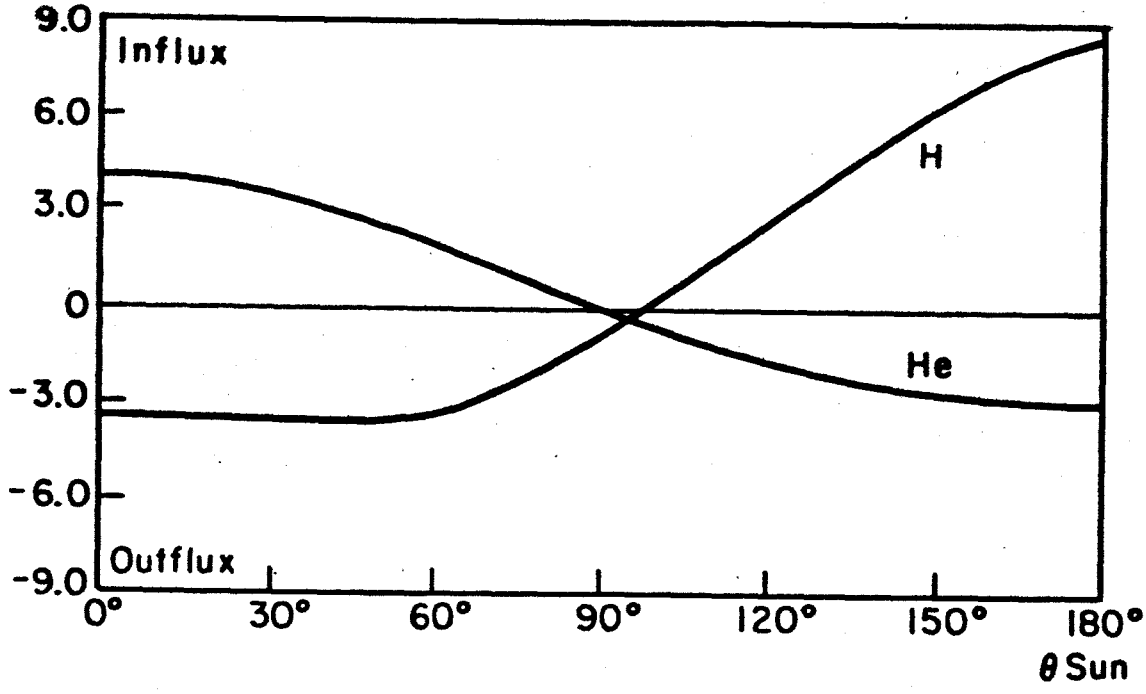

Fig. 10

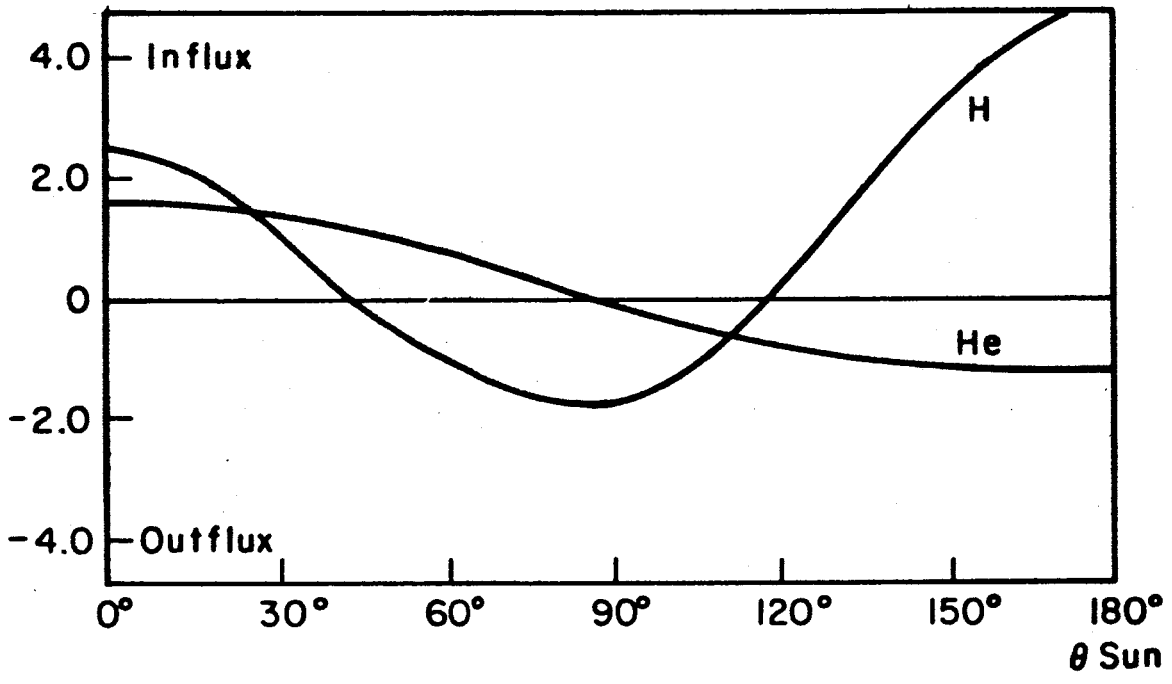

Fig. 11

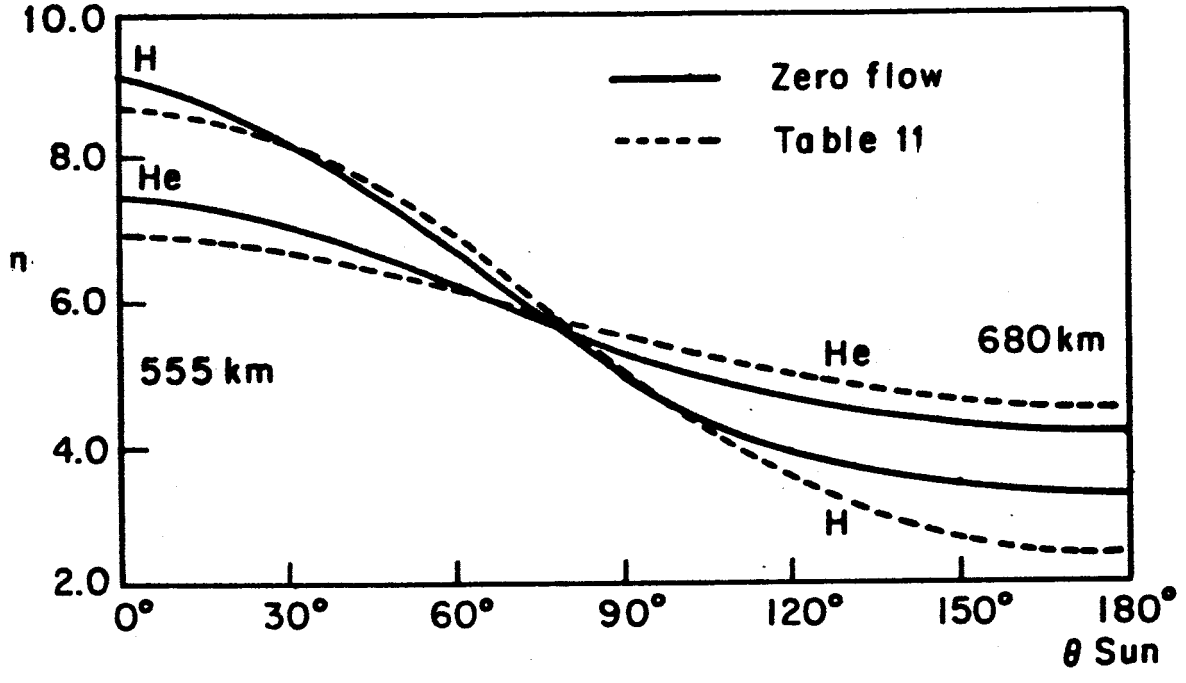
10.0
8.0
6.0
4.0
2.0
n
H
He
555 km
Zero flow
Table 11
He
680 km
H
0°
30°
60°
90°
120°
150°
180°
θ Sun

Fig. 12

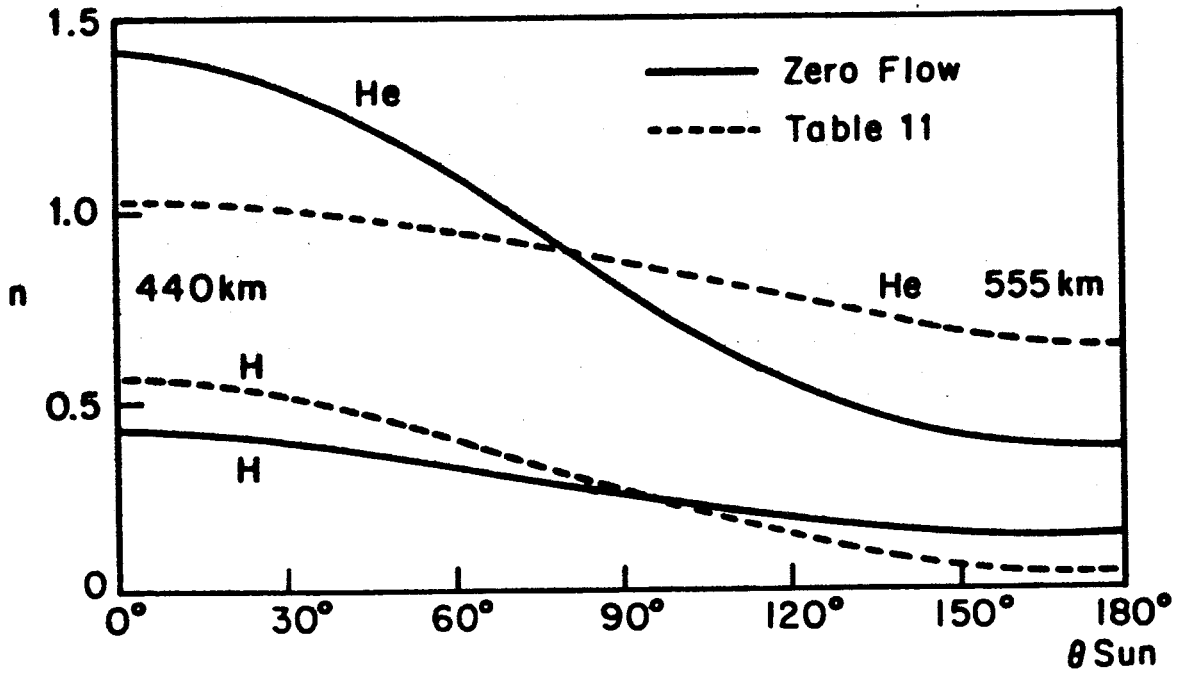
1.5
1.0
0.5
0
n
Zero Flow
Table 11
He
440km
He
555km
H
H
0°
30°
60°
90°
120°
150°
180°
θ Sun

Fig. 13

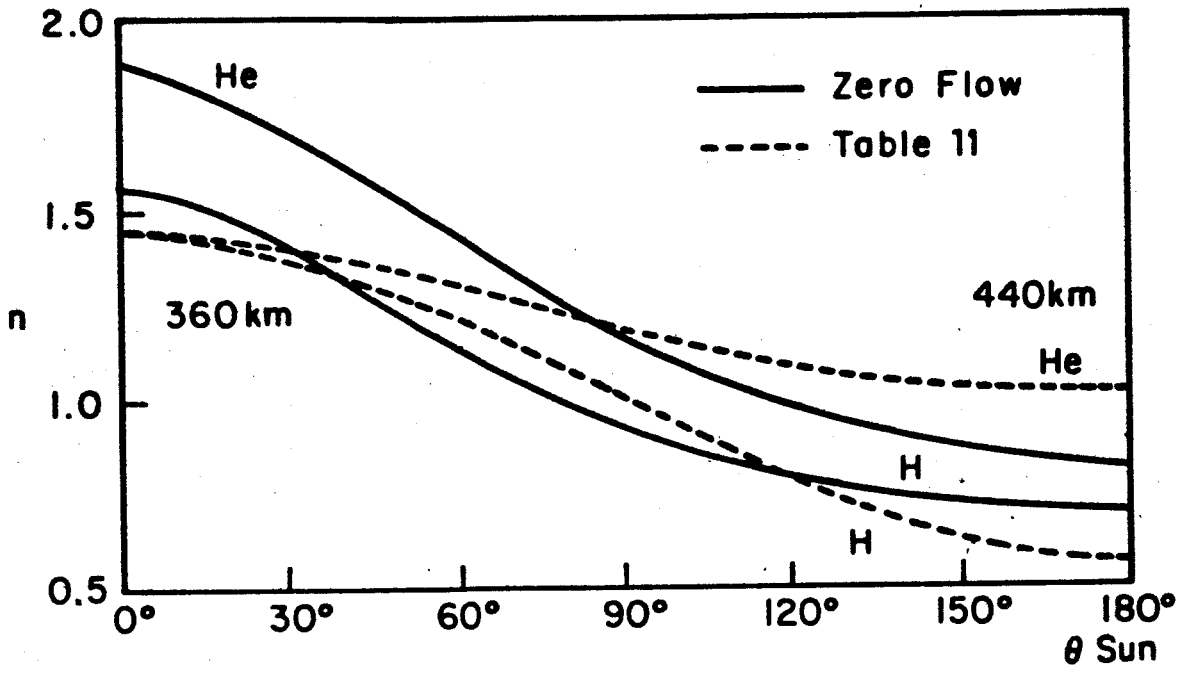
2.0
1.5
1.0
0.5
n
He
Zero Flow
Table 11
360km
440km
He
H
H
0°
30°
60°
90°
120°
150°
180°
θ Sun

Fig. 14

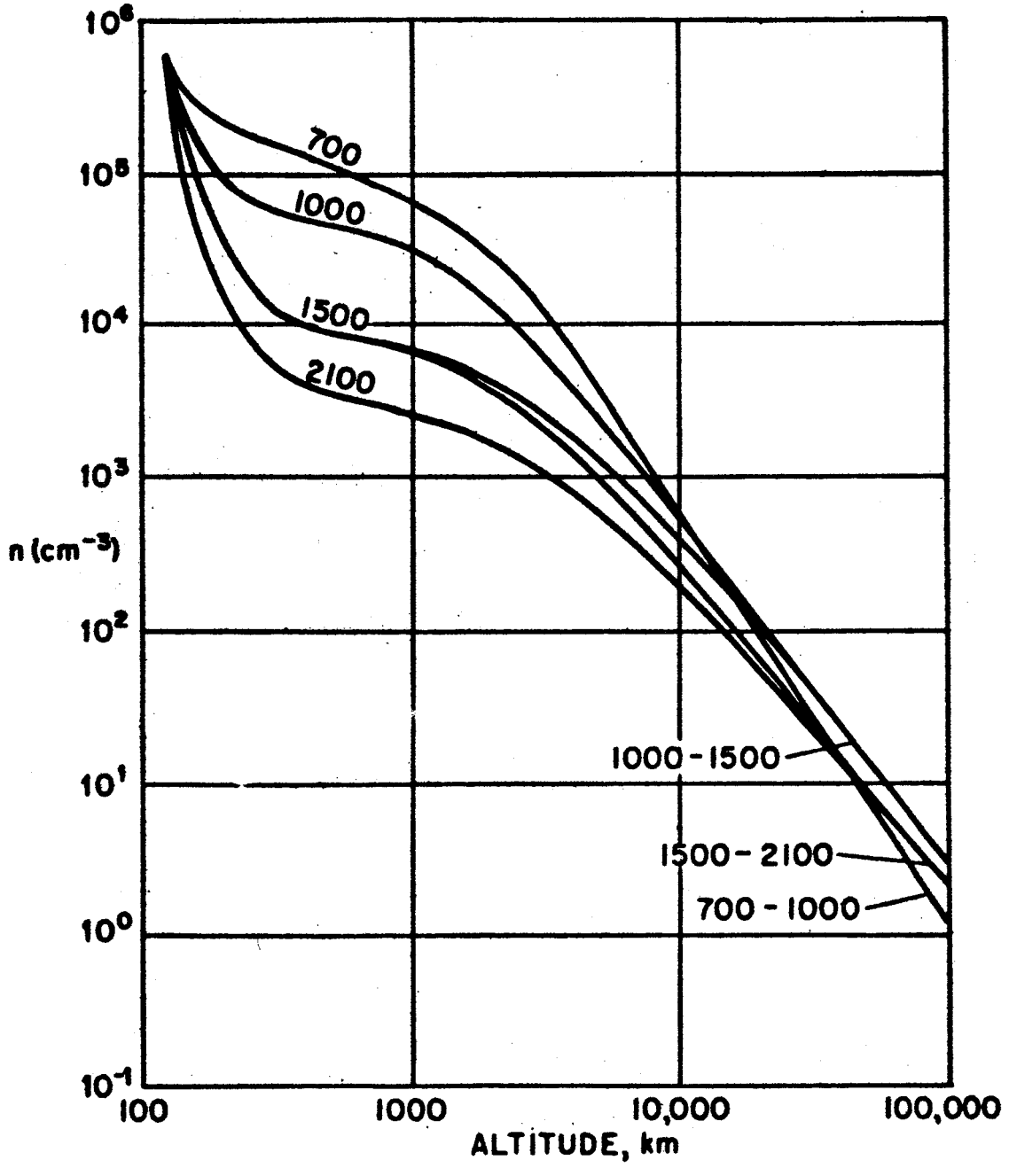
10^6
10^5
10^4
10^3
10^2
10^1
10^0
10^{-1}
n (cm^{-3})
700
1000
1500
2100
1000 - 1500
1500 - 2100
700 - 1000
100
1000
10,000
100,000
ALTITUDE, km

Fig. 15

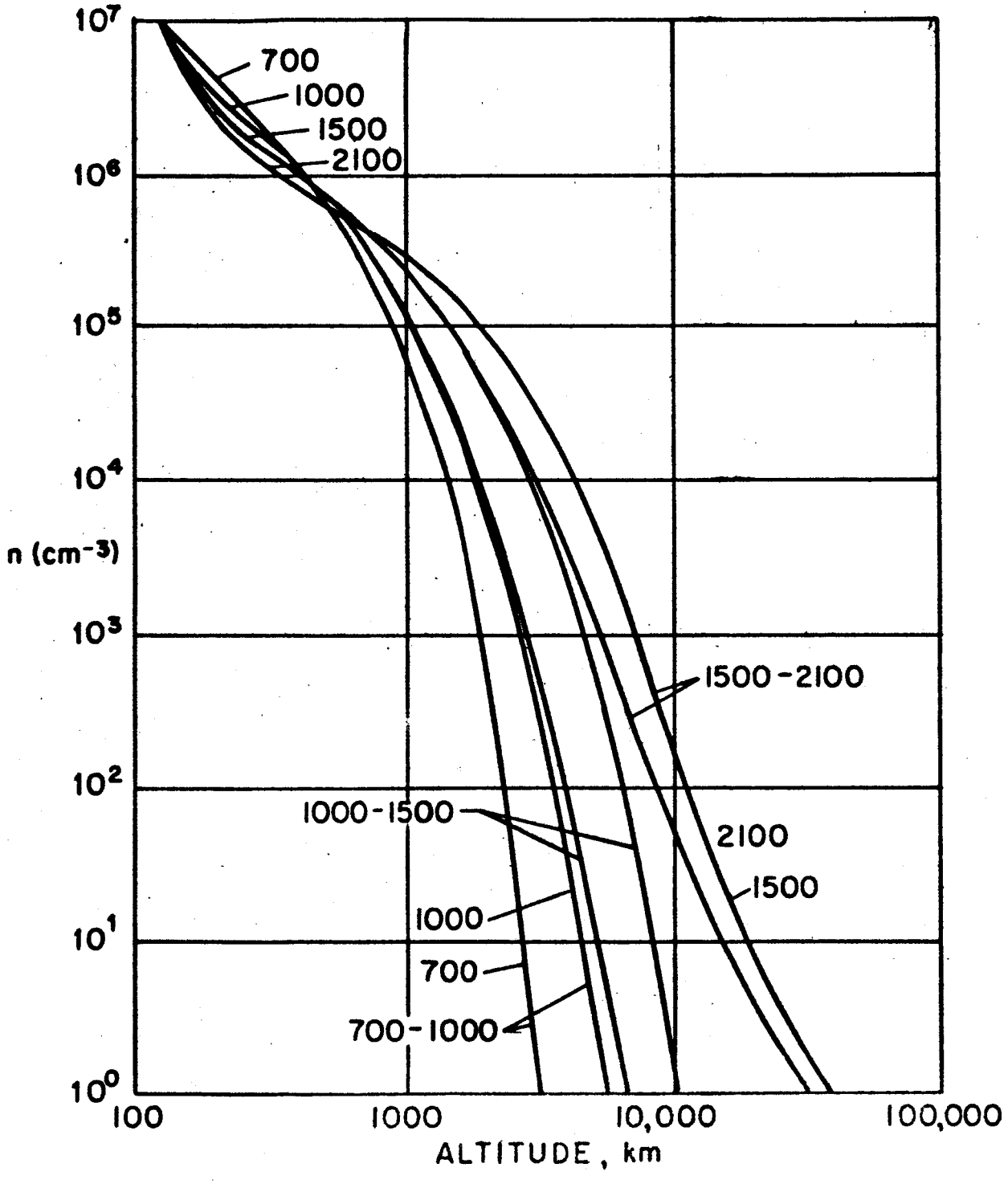
10^7
10^6
10^5
10^4
10^3
10^2
10^1
10^0
n (cm^{-3})
700
1000
1500
2100
1500-2100
1000-1500
2100
1500
1000
700
700-1000
100
1000
10,000
100,000
ALTITUDE, km

Fig. 16